PHASE SPACE TOMOGRAPHY DIAGNOSTICS AT THE PITZ FACILITY*

G. Asova†, S. Khodyachykh, M. Krasilnikov, F. Stephan, DESY, 15738 Zeuthen, Germany
P. Castro, F. Loehl, DESY, 22761 Hamburg, Germany

Abstract

A high phase-space density of the electron beam is obligatory for the successful operation of a Self Amplified Spontaneous Emission - FEL (SASE-FEL). Detailed knowledge of the phase space density distribution is thus very important for characterizing the performance of the used electron sources. The Photoinjector Test Facility at DESY in Zeuthen (PITZ) is built to develop, operate and optimise electron sources for FELs.

Currently a tomography module for PITZ is under design as a part of the ongoing upgrade of the facility.

This work studies the performance of the tomography module. Errors in the beam size measurements and their contributions to the calculated emittance are studied using simulated data. As a practical application the Maximum Entropy Algorithm (MENT) is used to reconstruct data generated by an ASTRA simulation.

INTRODUCTION

The current upgrade of the Photo Injector Test Facility at DESY in Zeuthen (PITZ) includes a tomography section for detailed analysis of the transverse phase-space density distribution of the electron beam. A simplified schematics of the beamline is shown in Fig. 1. It consists of a photo electron RF gun cavity (1), a low energy diagnostic section (2), followed by a further accelerating booster (3) and several elements of the high energy diagnostic section (4).

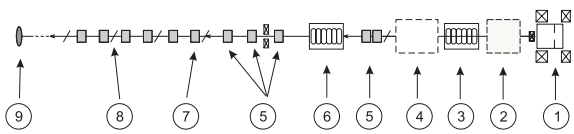

Figure 1: Simplified PITZ2 layout (not to scale). Single elements are described in the text.

The tomography module will consist of three pairs of FODO cells (7) and four diagnostic stations (8) for beam size measurements. An upstream matching section includes five quadrupoles (5) and is used to match the Twiss parameters for the designed energy. Both, the tomography and the matching sections, are designed in collaboration between CCLRC Daresbury Laboratory and DESY [1]. On a later stage it is foreseen to equip the tomography section with an RF deflecting cavity (6) to study the transverse emittance of longitudinal slices for selected electron bunches [2]. Total length of the matching section and the FODO lattice is designed to be 5.3 m starting at 9.1 m from the photocathode. The beamline continues with further diagnostics (not shown) and ends with a beam dump (9). Further details on the design considerations of the tomography section are given in [3].

This paper is structured as follows: the next section presents Monte Carlo simulations of beam emittance measurements and considerations taken into account for choosing betatron phase advance. Further, a reconstruction of an ASTRA [4] generated distribution with four transformations along the tomography module, having a phase advance of 45°, is demonstrated.

SIMULATIONS OF BEAM EMITTANCE MEASUREMENTS

There are several different ways to measure transverse emittance, e.g. slit technique [5] and the multi-screen method. The latter uses the knowledge of the beam sizes on different screens and the transport matrices between the screens to find the values of the beam sigma matrix $|\sigma_{ij}|$. The emittance is then calculated as

$$\epsilon = \sqrt{\sigma_{11}\sigma_{22} - \sigma_{12}^2}. \qquad (1)$$

In this section we study the contribution of spot size measurement errors to the calculated emittance. For this purpose Monte Carlo simulations were carried out using the method described in [6]. First the beam size and Twiss parameters for a periodic solution are calculated for the desired normalised emittance and phase advance in a FODO cell. For any seed in the simulation a random error with Gaussian distribution was added to the beam size. Extensive simulations were performed for different values of the betatron phase advance in a FODO cell in the region of 10° to 65°, normalised emittance 0.9π mm mrad, energy 32 MeV and beam size relative RMS error in the region 5% to 33%. The results are presented in Fig. 2 where the relative emittance measurement error is plotted as a function of the FODO phase advance for different relative beam size errors. As one can see from the plot the error decreases with phase advance having a minimum at around 45°.

For the phase advance of 45° we simulated 10000 measurements for a normalised emittance of 0.9π mm mrad and 10% relative beam size error. The results are presented in Fig. 3. The distribution indeed has a Gaussian shape with mean value of 0.9 and sigma of 0.09.

As one can see from equation (1) the emittance can be defined only if the expression under the square root is positive. Thus there is a finite probability to find no solution

* This work has partially been supported by the European Community, contract 011935 (EUROFEL)

† galina.asova@desy.de

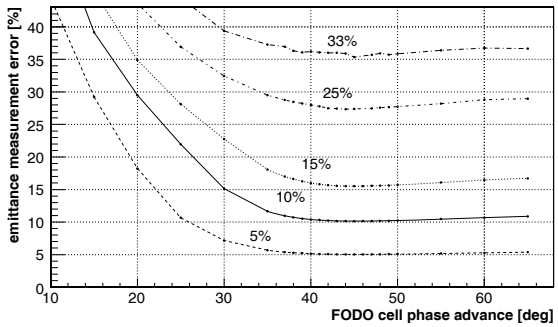

Figure 2: Emittance measurement error as function of phase advance for different beam size errors.

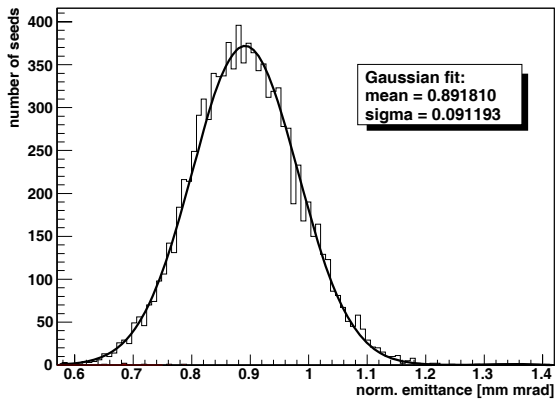

Figure 3: Emittance distribution for 0.9π mm mrad, phase advance 45° and relative beam size error 10%.

during measurement. Using the Monte Carlo simulations this probability was evaluated for different relative beam size errors. The results are shown in Fig. 4 together with relative emittance error. As one can see, for a relative beam size error smaller than 20% a solution can always be found. The probablity for no real solution increases then drastically with the growth of relative beam size error.

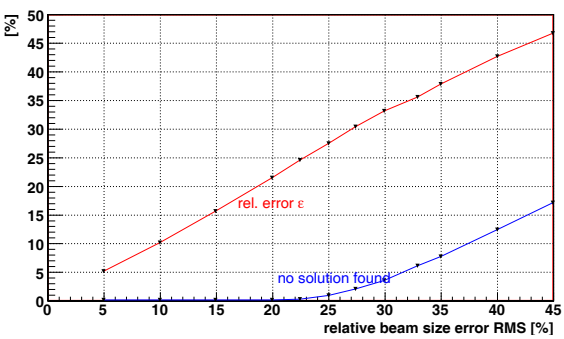

Figure 4: Rate of no solution and relative emittance error vs. relative beam size error for phase advance of 45°.

For the described reasons a phase advance of 45° in the FODO cell has been chosen. With a proper matching it delivers a periodic solution for particle trajectories in the lattice as shown in Fig. 5, where the β functions are plotted. The β functions were obtained using MAD–X with 32MeV total beam energy, a normalised emittance of 0.9π mm mrad and quadrupoles' strength delivering phase advance of 45°. Additionally ASTRA was running on 100000 particles, excluding space charge forces in the matching and tomography sections in order to obtain the beam sizes. For the periodic solution the values of the Twiss parameters at the sreens are α of -1.1436 and β of 1.00115 m.

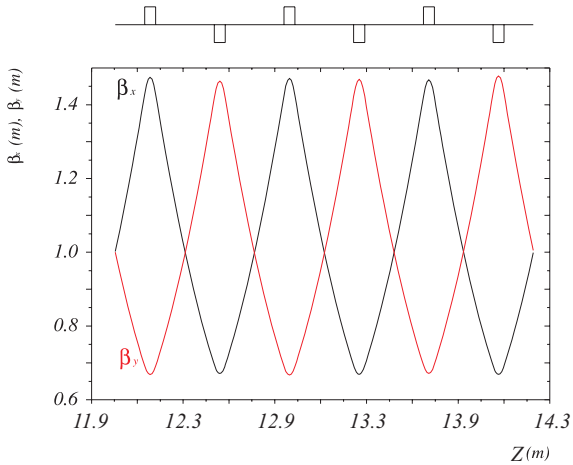

Figure 5: β functions along the tomography section.

TRANSVERSE PHASE SPACE RECONSTRUCTION

Detailed structure of the transverse phase space is necessary to be studied at a given location z along the beam line while making no assumptions about the distribution beforehand. Tomography techniques comprise the idea of reconstructing an image from a number of its spatial projections seen under different viewing angles. The objects of interest in the case of beam dynamics are two-dimensional functions $\rho(x, x')$ or $\rho(y, y')$, representing the beam density at position $z = z_{ini}$. The observed data are $f(x, y)$ distributions taken on N different screens, obtained by rotating the phase space ellipse with the help of quadrupole magnets in a number $(N - 1)$ predefined angular steps

$$\theta = \pi/N. \tag{2}$$

From each distribution a pair of projections, one for each axis, is taken according to

$$G_i(\theta, x_\theta) = \int f(x_\theta, y_\theta)\, dy_\theta, i = 1, \ldots, N \tag{3}$$

or

$$G_i(\theta, y_\theta) = \int f(x_\theta, y_\theta)\, dx_\theta, i = 1, \ldots, N. \tag{4}$$

Each projection at position $z = z_{obs}$ is mapped to a reference (x, y) frame at the position of the reconstruction using transverse phase space transformations between the screens or

$$\begin{pmatrix} x_\theta \\ y_\theta \end{pmatrix} = M_\theta \begin{pmatrix} x \\ y \end{pmatrix}. \quad (5)$$

M_θ is the transformation matrix between the first and each next observation position. In transverse phase space the spatial y_θ maps onto the divergence x' (y').

Minerbo's Maximum Entropy (MENT) algorithm [7] comprises minimum artefacts and is well suited in cases of noisy or incomplete data. It states that of all possible distribution functions $f(x, y)$ which satisfy the above equation, the solution is the most probable one in terms of entropy or in formula notation

$$H(x) = -\int\int f(x, y) \ln(f(x, y))\, dxdy. \quad (6)$$

By maximising the entropy - Eq. 6, from all possible solutions one selects the one that can be reproduced most often and is consistent with the information available from measurements. A detailed description of maximising the entropy is given in [8].

In the tomography section designed for PITZ the number of possible transformations of the phase space is three and correspondingly the number of projections is only four. Therefore, reconstruction algorithms which comprise minimum artefacts due to limited number of projections have to be employed. Currently the MENT algorithm is being investigated.

Transverse phase space distributions along the designed tomography module in both (x, x') and (y, y') planes at the position of the first screen, $z = 11.993$ m, have been generated with the ASTRA code using 100000 macroparticles. Influence from the space charge was not taken into account while tracking the particles through the matching section. The corresponding (x, y) distributions were used as an input for further investigations using the code presented in [9] which implements the MENT algorithm.

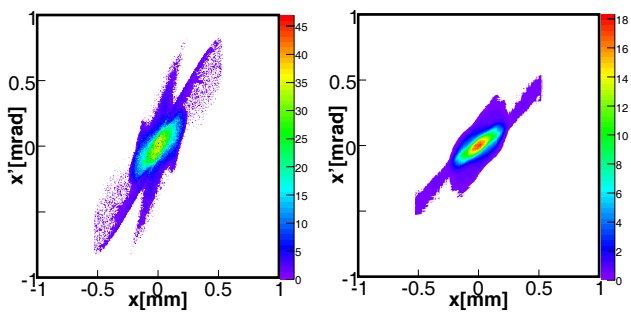

Figure 6: Original (left) and reconstructed (right) phase space in x plane.

Fig. 6 shows results of the (x, x') reconstruction obtained using the input projections plotted in Fig. 7. (y, y') reconstruction result is shown in Fig. 8.

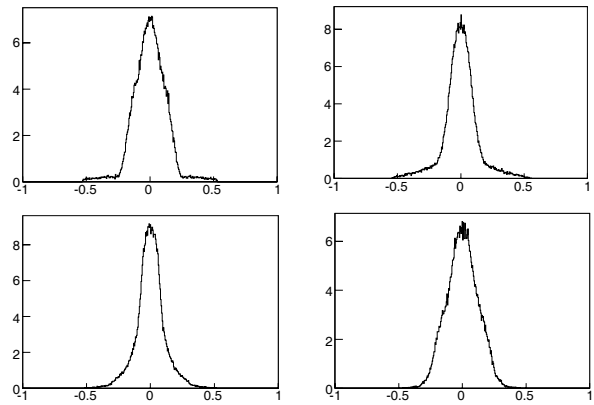

Figure 7: Profiles used in reconstruction of (x, x').

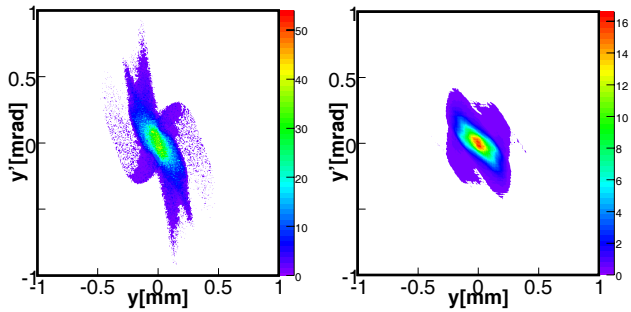

Figure 8: Original (left) and reconstructed (right) phase space in y plane.

Good agreement with respect to the slope of the phase space ellipse and the shape of its core is observed in both cases. The normalised emittance calculated from ASTRA is 0.986π mm mrad while from the reconstruction it is 0.967π mm mrad - the values agree within 2%. Other parameters of original and reconstructed phase space distributions are summarised in Table 1.

CONCLUSIONS

The present work studies how measurement errors influence the determination of beam emittance inside of the future tomography section of PITZ and shows an example of transverse phase space reconstruction. The MENT algorithm has to be developed further and its performance has to be evaluated against other tomography reconstruc-

Table 1: Beam size for original and reconstructed distribution at the first screen.

	$\mathbf{rms}_x$	$\mathbf{rms}_{x'}$	$\mathbf{rms}_{xx'}$	$\mathbf{rms}_y$	$\mathbf{rms}_{y'}$	$\mathbf{rms}_{yy'}$
original	0.13	0.2	0.0198	0.12	0.2	-0.015
recon.	0.14	0.2	0.023	0.11	0.19	-0.0124

tion techniques.

We would like to thank the members of the PITZ group for valuable discussions.

REFERENCES

[1] D.J. Holder et al., "A phase space tomography diagnostic for PITZ", proceedings of EPAC 2006, Edinburgh, UK.

[2] S. Korepanov at al.,"Design Consideration of the RF Deflector for PITZ", to be published in proceedings of FEL 2006, Berlin, Germany.

[3] D.J. Holder et al., "Design of a Phase Space Tomography Module", EuroFEL report, to be pulished.

[4] ASTRA: A Space Charge Tracking Algorithm, http://www.desy.de/˜mpyflo/.

[5] V. Miltchev, "Investigations on the Transverse Phase Space at a Photo Injector for Minimised Emittance", PhD thesis, Humboldt University, Berlin, Germany (2006).

[6] P. Castro, "Monte Carlo Simulations of emittance measurements at TTF2", DESY Technical Note 03-03.

[7] G. Minerbo, "A Maximum Entropy Algorithm for Reconstructing a Source from Projected Data", Comp. Graphics Image Proc. 10 (1970) 48.

[8] C.T. Mottershead, "Maximum Entropy Beam Diagnostic Tomography", IEEE Trans. Nucl. Sci. Vol. NS-32 (1985) 1970.

[9] J.J. Scheins, "Tomographic Reconstruction of Tranverse and Longitudinal Phase Space Distribution using Maximum Entropy Algorithm", TESLA Report 2004-08.